Quantitative measurement and interpretation of optical second harmonic generation from molecular interfaces

Wen-kai Zhang,† Hong-fei Wang* and De-sheng Zheng†

Received 6th June 2006, Accepted 13th July 2006
First published as an Advance Article on the web 2nd August 2006
DOI: 10.1039/b608005g

Second harmonic generation (SHG) has been proven a uniquely effective technique in the investigation of molecular structure and conformations, as well as dynamics of molecular interfaces. The ability to apply SHG to molecular interface studies depends on the ability to abstract quantitative information from the measurable quantities in the actual SHG experiments. In this review, we try to assess recent developments in the SHG experimental methodologies towards quantitative analysis of the nonlinear optical properties of the achiral molecular interfaces with rotational isotropy along the interface normal. These developments include the methodology for orientational analysis of the SHG experimental data, the experimental approaches for more accurate SHG measurements, and a novel treatment of the symmetry properties of the molecular polarizability tensors in association with the experimentally measurable quantities. In the end, the recent developments on the problem of surface *versus* bulk contribution in SHG surface studies is discussed. These developments can put SHG on a more solid foundation for molecular interface studies, and to pave the way for better understanding and application of SHG surface studies in general.

1. Introduction

Second harmonic generation (SHG) is the second order nonlinear process where two photons with the same fundamental frequency (ω) interact with a nonlinear medium simultaneously to generate a photon with the second harmonic frequency (2ω). If the two fundamental frequencies are not the same, a photon at the sum of these two frequencies can be generated from the so-called sum frequency generation (SFG) process. Because of the symmetry requirement for the second order nonlinear processes, the leading dipolar term of the SHG or SFG processes is generally forbidden for the centrosymmetric bulk medium, and thus SHG and SFG become effective probes for the surface of the centrosymmetric bulk phase.[1] Since Shen and his colleagues laid the theoretical foundation and demonstrated the experimental feasibility of SHG and SFG for surface studies with submonolayer level sensitivity,[2–7] surface second harmonic generation (SSHG) and SFG have been used as powerful probes for structural and spectroscopic information of the molecular interfaces and molecular thin films in the past two decades.[8–17] SSHG has also become one of the most important tools for liquid and material surface characterizations.[15–27] SSHG has also been used to probe molecular electronic spectroscopy of molecular interfaces.[3,28–31] There have been a number of books or book chapters,[32,33] and review articles[9–17] on the fundamental theory and different aspects of the applications for surface studies with SSHG over the past twenty years. Some new developments of SHG techniques, including SHG from micro- and nano-particle surfaces,[34–36] second harmonic microscopy (SHM),[37–39] SHG chirality studies, such as SHG circular dichroism (SHG-CD), SHG linear dichroism (SHG-LD) and SHG optical rotatory dispersion (SHG-ORD)[40–42] have also been reviewed recently.

The ability to apply SHG, as well as SFG, in molecular interfaces depends on the ability to abstract quantitative information from the measurable quantities in the actual SHG or SFG experiments. In recent years, Zhuang *et al.* introduced a unified approach to employ SHG and SFG for mapping molecular orientation and conformation at interfaces,[43] while Simpson *et al.* presented a unified treatment on the selection rules and symmetry relations for SHG and SFG spectroscopies.[44,45] These efforts are certainly very useful and educational in SHG and SFG studies. However, conducting quantitative interpretation of the SHG or SFG data is still not as straightforward as it appears, and it has not been a simple trade. It is still difficult for those who want to employ them, especially because the techniques and methodologies for measuring and interpreting the SHG and SFG data have been scattered in various literatures, and need to be systematically developed and summarized.

Recently, we systematically discussed some recent developments in methodologies and issues involved in quantitative spectral and orientational analysis in the sum frequency generation vibrational spectroscopy (SFG-VS).[8] The key idea in these developments is to directly connect the microscopic second order polarizability tensor elements to the polarization and experimental configuration dependent SFG-VS measurable quantities through molecular symmetry analysis. We

State Key Laboratory of Molecular Reaction Dynamics, Institute of Chemistry, Chinese Academy of Sciences, ZhongGuanCun, Beijing, China 100080. E-mail: hongfei@iccas.ac.cn; Fax: 86-10-62563167
† Also Graduate University of the Chinese Academy of Sciences.

further demonstrated that polarization and experimental configuration analysis of the SFG-VS data can be used to elucidate complex vibrational spectral features and molecular structures for various molecular interfaces.[46–49]

A similar analysis can also be employed in SHG analysis, except that it is more complicated for SHG analysis than that for SFG-VS. Therefore, SHG has been generally considered a less specific technique than SFG.[50] This is simply because, unlike in SFG-VS,[8] most SHG measurements are not right on the electronic resonance, and that there is no simple way to separate the contributions to the measured SHG signal from the symmetric and asymmetric polarizability tensor elements in the analysis. In the SHG literatures, simplification of the molecular polarizability tensor elements with uniaxial or rod-like assumption was generally used,[21–25] except for a few cases.[16,43,51–53] Nevertheless, a systematic and unified treatment of the molecular tensor elements can be very helpful in understanding and application of the SHG for surface and thin film studies.

The objective of this short review is to examine the issues and techniques for quantitative measurement and interpretation of SHG data from the molecular interfaces and thin films. We limit our scope to the achiral molecular interfaces with rotational isotropy along the interface normal. We are particularly interested in the so-called "inverse problem", which is to use the results of actual SHG measurements to infer the unique values of the parameters directly from the fundamental theory of SHG, which characterize the molecular interface and thin films. Scientifically, to predict the SHG experimental observations with given values of the parameters, *i.e.* the so-called "normal problem", *i.e.*. "forward problem", is nevertheless meaningful, but may not be as challenging and important as to solve the "inverse problem". By addressing these issues, experimental studies and interpretations of SHG may be carried out within a relatively unified framework.

In the following sections, we shall discuss the methodologies for orientational analysis of the SHG experimental data, discuss the experimental approaches for more accurate SHG measurements, and then present a novel treatment of the symmetry properties of the molecular hyperpolarizability tensors in association with the experimentally measurable quantities. In the end, a recent development on the problem of surface *versus* bulk contribution in SHG surface studies is presented. We hope that this review can put SHG on a more solid foundation for molecular interface studies, and also pave the way for better understanding and application of SHG for surface studies in general.

2. Basic theory for SHG

The basic theory of SHG as a general surface analytical probe has been well described in the literature.[11,43,54–56]

Generally, the SHG intensity $I(2\omega)$ reflected from an interface is given below.[43]

$$I(2\omega) = \frac{32\pi^3\omega^2\sec^2\Omega}{c_0^3 n_1(\omega)n_1(\omega)n_1(2\omega)}|\boldsymbol{\chi}_{\text{eff}}|^2 I_\omega^2 \qquad (2.1)$$

$$\boldsymbol{\chi}_{\text{eff}} = [\mathscr{L}(2\omega):\hat{\boldsymbol{e}}(2\omega)]\cdot\boldsymbol{\chi}:[\mathscr{L}(\omega):\hat{\boldsymbol{e}}(\omega)]\cdot[\mathscr{L}(\omega):\hat{\boldsymbol{e}}(\omega)] \qquad (2.2)$$

In eqn (2.1), I_ω is the incoming laser intensity, c_0 is the speed of the light in the vacuum, and Ω is the incident angle from the surface normal. In eqn (2.2), $\boldsymbol{\chi}$ is the macroscopic second-order susceptibility tensor, which has $3 \times 3 \times 3 = 27$ elements; $\hat{\boldsymbol{e}}(2\omega)$ and $\hat{\boldsymbol{e}}(\omega)$ are the unit vectors of the electric field at 2ω and ω; $\mathscr{L}(2\omega)$ and $\mathscr{L}(\omega)$ are the tensorial Fresnel factors for 2ω and ω, respectively.

It is important to realize that $\boldsymbol{\chi}_{\text{eff}}$ contains all molecular information of SHG measurement. $\boldsymbol{\chi}_{\text{eff}}$ is generally complex, and both an amplitude and a phase factor are required to quantify it. Generally, in many cases there is no relative phase between the different $\boldsymbol{\chi}_{\text{eff}}$ terms, and these $\boldsymbol{\chi}_{\text{eff}}$ terms can be treated as real values in the interpretation of SHG data. In fact, any $\boldsymbol{\chi}_{\text{eff}}$ in SHG can be expressed into the linear combination of a few non-zero independent experimentally measurable $\boldsymbol{\chi}_{\text{eff}}$ terms in specific polarization combinations.

For example, there are three independent $\boldsymbol{\chi}_{\text{eff}}$ terms for an achiral rotationally isotropic interface ($C_{\infty v}$), namely, s-in/p-out ($\boldsymbol{\chi}_{sp}$), 45°-in/s-out ($\boldsymbol{\chi}_{45°s}$) and the p-in/p-out ($\boldsymbol{\chi}_{pp}$). Here, in the experimental coordinate system (x,y,z), z is the interface normal, and we choose the xz plane to be the incident plane. Subsequently, p polarization is defined as polarization within the xz plane, and s is perpendicular to the xz plane. These $\boldsymbol{\chi}_{\text{eff}}$ terms are directly related to the interfacial macroscopic susceptibilities χ_{ijk} tensor elements as the following:[43,57]

$$\begin{aligned}
\boldsymbol{\chi}_{\text{eff},sp} &= L_{zz}(2\omega)L_{yy}^2(\omega)\sin\Omega\chi_{zyy}\\
\boldsymbol{\chi}_{\text{eff},45°s} &= L_{yy}(2\omega)L_{zz}(\omega)L_{yy}(\omega)\sin\Omega\chi_{yzy}\\
\boldsymbol{\chi}_{\text{eff},pp} &= L_{zz}(2\omega)L_{xx}^2(\omega)\sin\Omega\cos^2\Omega\,\chi_{zxx}\\
&\quad - 2L_{xx}(2\omega)L_{zz}(\omega)L_{xx}(\omega)\sin\Omega\cos^2\Omega\chi_{xzx}\\
&\quad + L_{zz}(2\omega)L_{zz}^2(\omega)\sin^3\Omega\chi_{zzz}
\end{aligned} \qquad (2.3)$$

in which the Fresnel factor $L_{ii}(\omega)$ terms were clearly defined by Zhuang and Wei *et al.*[43,57] However, there can be up to 6 non-zero independent measurable $\boldsymbol{\chi}_{\text{eff}}$ terms for interfaces or films with symmetry other than $C_{\infty v}$.[58]

One can show that $\boldsymbol{\chi}_{\text{eff}}$ in any experimental configuration with linearly polarized light can be directly expressed into the linear combination of these three independently measurable $\boldsymbol{\chi}_{\text{eff}}$ terms as in eqn (2.4). Cases other than those using linearly polarized light shall be discussed in section 4.

$$\begin{aligned}
\boldsymbol{\chi}_{\text{eff}} &= \sin^2\alpha\cos\gamma\boldsymbol{\chi}_{\text{eff},sp} + \sin 2\alpha\sin\gamma\boldsymbol{\chi}_{\text{eff},45°s}\\
&\quad + \cos^2\alpha\cos\gamma\boldsymbol{\chi}_{\text{eff},pp}
\end{aligned} \qquad (2.4)$$

Here, α and γ are the polarization angle measured from the optical plane of the incident laser beam and the detection polarization angle in the outgoing signal beam, respectively.

Generally, χ_{ijk} is the ensemble orientational average of the second order molecular polarizability tensor elements $\beta_{i'j'k'}$ in the molecular system.[33]

$$\chi_{\text{ijk}} = N_s\sum_{i'j'k'=abc}\langle R_{ii'}R_{jj'}R_{kk'}\rangle\beta_{i'j'k'} \qquad (2.5)$$

where N_s is the molecule number density, the operator $\langle\rangle$ denotes the orientational ensemble average over the Euler rotation matrix transformation element $R_{\lambda\lambda'}$ from the molecular coordinate $\lambda'(a,b,c)$ to the laboratory coordinate $\lambda(x,y,z)$,[59] through the three Euler angles (θ,ψ,φ).[60] The

subscript (i,j,k) of the χ_{ijk} corresponds to the laboratory coordinate (x,y,z), and the subscript (i',j',k') of the $\beta_{i'j'k'}$ corresponds to the molecular coordinate (a,b,c). Here in eqn (2.5), the convention to incorporate the local field factors into an effective refractive index is followed.[43]

For a rotationally isotropic achiral molecular interface or thin film, there are only 7 non-zero χ_{ijk} tensor elements, *i.e.* χ_{zzz}, $\chi_{zxx} = \chi_{zyy}$, $\chi_{yzy} = \chi_{yyz} = \chi_{xzx} = \chi_{xxz}$.[61] These relationships are generally valid when there are more than one kind of molecular species contributing to the macroscopic susceptibilities. Because the rotational average in eqn (2.5) is independent of frequency, χ_{ijk} and $\beta_{i'j'k'}$ should have the same frequency response. Therefore, measurement of the frequency dependence of χ_{ijk} also provides the spectrum of the interface molecule. This fact has been used to measure the interface polarity of the liquid interfaces using polarity indicator molecules.[29,30]

Based on the above, a schematic for SHG studies of interfaces or thin films is illustrated in Fig. 1.[8,62] Just as Corn and Higgins have summarized,[16] SHG molecular orientation measurement incorporates three main steps. It is clear that the first step is to accurately measure the non-zero independent $\boldsymbol{\chi}_{\text{eff}}$ terms. A lot of work has been done in order to determine the relative magnitudes and phases of these $\boldsymbol{\chi}_{\text{eff}}$ terms.[63–65] The second step is to calculate or assume the $\beta_{i'j'k'}$ terms of an individual molecule. And third, the average molecular orientation at the interface should be calculated through the appropriate equations which relate the experimentally measured $\boldsymbol{\chi}_{\text{eff}}$ terms to the microscopic $\beta_{i'j'k'}$ terms.

The second step is crucial since there are only a limited number (generally three) of non-zero independent $\boldsymbol{\chi}_{\text{eff}}$ terms can be measured. It is also where confusion arises and disagreements diverge. In practice, a rod-like approximation, *i.e.* β_{ccc} is the only non-zero term, is usually used, and the analysis is greatly simplified.[21–25] However, such approximation may not be suitable for the typical rod-like chromophore in the molecules, such as in 4′-*n*-octyl-4-cyanobiphenyl (8CB).[43,53] *Ab initio* or other theoretical calculations have also been used to calculate the molecular $\beta_{i'j'k'}$ terms.[66,67] However, such an approach is intrinsically limited because it requires calculation and summation over the electronically excited states. As illustrated in Fig. 1, recent developments have shown that symmetry analysis in SHG at interface and in hyper-Rayleigh scattering (HRS) in solution can be used to simplify and experimentally determine the ratios between the molecular $\beta_{i'j'k'}$ terms. HRS can be employed for SHG studies here simply because HRS is basically the incoherent aspect of the second order nonlinear optical process, while SHG is the coherent aspect of the same second order nonlinear process.[68,69] These development shall be discussed in detail in section 5.

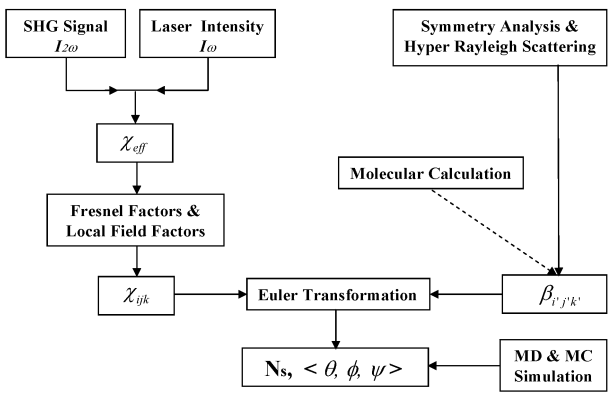

Fig. 1 Schematic illustration of SHG quantitative analysis. Adapted on the basis of the illustration by C. D. Bain on SFG-VS analysis.[8,62]

It should be noted that above discussions are valid both for molecular interfaces and thin films. In the following sections, we shall discuss issues related to recent advances on quantitative measurement and interpretation of SHG from molecular interfaces and thin films.

3. Methodology for quantitative orientational analysis

Recently the limitations of using SHG for molecular orientational analysis of molecular interfaces and thin films have been seminally discussed by Simpson and Rowlen.[12,13,70] In these works, Simpson and Rowlen demonstrated that because each apparent orientational angle from the SHG measurement actually corresponds to a broad range of possible orientational angle and distribution widths of the molecules at the interface, it is impossible to determine the molecular orientational angle and distribution width solely using the SHG polarization measurement. Simpson and Rowlen further discussed the idea of orientationally insensitive measurement of molecular interfaces and thin films with SHG.[71,72] However, there are also clear advantages of using nonlinear and coherent spectroscopic techniques, such as SHG and SFG-VS, for molecular orientational analysis of molecular interfaces and thin films, especially with the formulation of orientational functional and general orientational parameters.[8,54,56,59,73]

3.1. The orientational parameter and the SHG "magic angle"

In SHG surface studies, the orientational parameter $D = \langle\cos\theta\rangle/\langle\cos^3\theta\rangle$, which can be experimentally determined from polarization or null angle measurements, was generally used to determine the interface orientational angle and distribution width.[4,33,54] In early studies, a very narrow or δ-distribution approximation, *i.e.* $\sigma = 0^\circ$, was generally assumed, and an apparent orientational angle (θ_a) was readily calculated. However, such a simplification is usually problematic, especially for rough surfaces where adsorbed molecules are likely to have a broad angular distribution. Simpson and Rowlen explicitly discussed the limitations of using D parameter only to determine the orientational angle and distribution width of molecular interfaces and thin films.[12,13,70] These limitations are based on the existence of the "magic angle" in the analysis of mathematical expression of the D parameter, as illustrated in Fig. 2.[70]

It is obvious that with a single value of D, it is impossible to simultaneously determine two independent orientational variables, namely, the orientational angle (θ) and distribution width (σ). When $D = 5/3$, $\theta_a = 39.2^\circ$ is called the "magic angle" because any orientational center angle (θ) with a certain broad distribution width (σ) can satisfy this D value. To

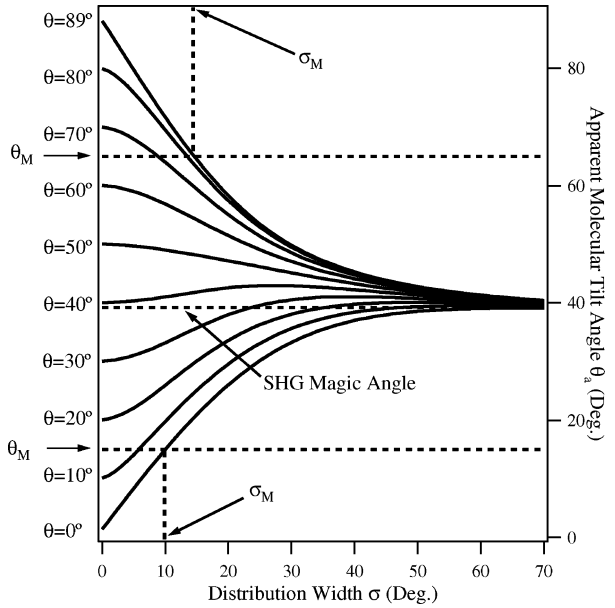

Fig. 2 The apparent molecular orientational angle (calculated by assuming a δ-function distribution) as a function of the root-mean-square width σ of a Gaussian distribution function. Each curve corresponds to a center orientational angle θ. The straight line at 39.2° is the magic angle. Two horizontal dashed lines are drawn to show how to determine the θ_M and σ_M with known D value as discussed in the text. Adapted with permission from G. J. Simpson and K. L. Rowlen, *J. Am. Chem. Soc.*, 1999, **121**, 2635–2636. Copyright 1999 American Chemical Society.[70]

resolve this fundamental limitation, Simpson and Rowlen demonstrated a way using the orientational parameter $K = \langle\cos^2\theta\rangle$ obtained from some thin film sensitive linear polarization spectroscopic techniques, such as the angle-resolved absorbance by photoacoustic detection (APARD) technique, together with the D parameter obtained from SHG measurement, to uniquely determine both θ and σ for molecular interfaces or thin films.[74] However, the key difficulty in this approach is that the linear measurement cannot satisfy the monolayer sensitivity required for most of these cases. In order to deal with the limitation of the single D value method and to keep the advantage of the submonolayer sensitivity of SHG, recently a SHG only approach was proposed and demonstrated by Rao *et al*. based on the analysis of the orientational functional in SHG defined below.[56]

One direct extension of the analysis of the "magic angle" in Fig. 2 is that with any D value, provided it is accurately measured, a maximum or minimum possible orientational angle θ_M and a maximum possible distribution width σ_M can be easily determined. This information is especially useful when D value is significantly away from the "magic angle" value of $D = 5/3$ in SHG and SFG-VS measurements.[75–77] In these cases, σ_M can be relatively small, *i.e*. a relatively narrow distribution width is ensured.

3.2. Orientational analysis with the orientational functional

The advantages of orientational analysis with nonlinear and coherent spectroscopic methods were demonstrated through a simplified formulation of the orientational functional $R(\theta)$ for both linear and nonlinear spectroscopic techniques in the study of ordered molecular systems, including molecular interfaces and thin films.[59] For example, since all the non-vanishing third order macroscopic χ tensor elements in SHG or SFG-VS are just linear function of $\langle\cos\theta\rangle$ and $\langle\cos^3\theta\rangle$ terms, any χ_{eff} can be simplified into[56]

$$\chi_{eff} = N_s d(\langle\cos\theta\rangle - c\langle\cos^3\theta\rangle) = N_s d r(\theta). \quad (3.6)$$

Therefore,

$$I(2\omega) = A d^2 R(\theta) N_s^2 I_\omega^2 \quad (3.7)$$

$$R(\theta) = |r(\theta)|^2 = |\langle\cos\theta\rangle - c\langle\cos^3\theta\rangle|^2 \quad (3.8)$$

Here, A is a proportional constant, and $R(\theta)$ is called the orientational functional. $R(\theta)$ solely depends on the general orientational parameter c, which is a dimensionless number. Therefore, the SHG intensity $I(2\omega)$ is directly proportional to $d^2R(\theta)$, in which the orientational functional $R(\theta)$ contains all the molecular orientational information. The strength factor d, with the unit of molecular polarizability β, determines the magnitude of $I(2\omega)$.[56] According to the definition, c and d are the functions of the relative ratios of the molecular polarizability tensors, the incident and outgoing angles, the polarization angles, and the dielectric constants of the two bulk media and the molecular layer in both the fundamental and second harmonic light frequencies. The full expressions for the c and d values of the uniaxial molecular systems with a rotational isotropic along the surface normal in different SHG experimental configurations are given in the literature.[56] Expressions for c and d values in SFG-VS are also available for methyl groups.[47]

Such separation of the orientational response $R(\theta)$ and strength factor d is the key for explicit orientational analysis in recent SHG and SFG-VS studies.[8,46–49,56,59,75–77] Systematic simulation of the behavior of $R(\theta)$ with different c values provided rich information and detailed understanding of the orientational response of $I(2\omega)$. From these expressions of c, one can show that by changing the SHG experimental incident angles, the incident and outgoing polarizations angles, c value can be changed from $-\infty$ to ∞. This fact enables full experimental control of the measurements with different c values for SHG orientational analysis.[56]

Undoubtedly, the value of c controls the behavior of $R(\theta)$ against possible molecular orientation and distributions. Therefore, c is the true orientational parameter. Here c is called the general orientational parameter because when $R(\theta) = 0$, the corresponding c value becomes the orientational parameter D. With the c and D values, $r(\theta)$ is directly connected to the first and the third orientational order parameters through the following relationship,[56]

$$r(\theta) = (1 - \frac{c}{D})\langle\cos\theta\rangle = (1 - \frac{c}{D})S_1 = (D - c)\langle\cos^3\theta\rangle = \frac{1}{5}(D - c)(2S_3 + 3S_1) \quad (3.9)$$

in which $S_1 = \langle\cos\theta\rangle$, and $S_3 = (5\langle\cos^3\theta\rangle - 3\langle\cos\theta\rangle)/2$ are the first and the third *orientational order parameters* of the system. So the deviation of c from the orientational parameter c_0, or D, scales the value of the orientational response, *i.e*. $r(\theta)$,

of the molecular system. This relationship entrust clear physical meaning to c as the so-called *general orientational parameter*.

A clear demonstration of the $R(\theta)$ analysis is in Fig. 3. Without the analysis with $R(\theta)$, the SHG experimental observation of the complex orientational phase behaviors of the Langmuir film of the liquid crystal molecule 8CB at the air/water interface could not have been clearly understood.[56] Using the known experimental condition and molecular parameters, the c values of the 8CB Langmuir monolayer in the three independent experimental polarization configurations are:[56] $c = 1$ for s-in/p-out (*sp*) and 45°-in/s-out (45°*s*), and $c = 2.25$ for p-in/p-out(*pp*). With these c values, orientational analysis on $R(\theta)$ can draw the following conclusions:[56]

(a) With the same c value, the *sp* and 45°*s* SHG curves undoubtedly have the same orientational behavior.

(b) The behavior of the *sp*, 45°*s* and *pp* SHG curves in region II can only be explained by a continuous tilting and narrowing orientational phase transition process. This process ends at the starting point of region III, which fits well with the sharp turning point on the surface pressure curve. This explicitly indicates that the sharp turn on the surface pressure curve at 52 Å^2 can not be a simple first-order orientational phase transition.[78,79] Furthermore, the θ and σ of the diphenyl chromophore of 8CB molecule can be directly calculated for region II using the SHG data in different polarizations and surface densities.

(c) The different trend in the *sp*, 45°*s*, and *pp* SHG curves in region III can be easily explained by the shadowed region of the $R(\theta)$ curves with $c = 1$ and $c = 2.25$ in Fig. 3b, because only in this region did the $c = 1$ curve change little with the tilt angle θ, while the $c = 2.25$ curve changed proportionally with the same tilt angle change. Quantitative calculation just confirms this direct observation with the corresponding $R(\theta)$ curves. This explicitly demonstrate the power of the $R(\theta)$ orientational analysis.

Further examination of the behavior of $R(\theta)$ in Fig. 3b also reveals the following simple but important conclusions:

(a) When $c = 1$, $R(\theta)$ goes to zero at $\theta = 0°$ and $\theta = 90°$. This directly contradicts the belief that more SHG signal should be observed when the chromophore is more upright.[80–82]

(b) $R(\theta)$ curves with different c values possess orientational sensitive and orientational insensitive regions. Therefore, they can be used for orientational sensitive and orientational insensitive measurements of the chromophore orientation and orientational changes through tuning of the c values with controlled experimental configurations, including incident angles and polarization angles. Simpson and Rowlen demonstrated the idea to make an orientational insensitive measurement with SHG for the first time.[71,72] Here the formulation of the orientational functional $R(\theta)$ provides a convenient toolbox for conducting both orientational sensitive and insensitive measurements in SHG and SFG-VS. Following this idea, an orientational sensitive measurement of the 3700 cm^{-1} free O–H vibrational peak at an air/water interface in the *ppp* polarization has shown two orders of magnitude intensity change with different incident angles of the laser beams, while only 20–30% change was observed in the *ssp* polarization with the same set of incident angles. This has greatly helped discern the symmetry and orientation angle of this free O–H bond at the air/water interface.[48,49]

Orientational analysis with $R(\theta)$ provides a way to simultaneously determine both θ and σ by using SHG measurements with different c values. This approach was explicitly formulated and demonstrated for the 8CB Langmuir monolayer studies.[56] Conceptually, such task can be realized if one can measure two independent $r(\theta)$ values from SHG experimental measurements under two different c values.[56]

$$r_1(\theta) = \langle \cos\theta \rangle - c_1 \langle \cos^3\theta \rangle \quad (3.10)$$

$$r_2(\theta) = \langle \cos\theta \rangle - c_2 \langle \cos^3\theta \rangle \quad (3.11)$$

Thus, two independent measurements provide a unique solution for the two orientational variables θ and σ, provided that the two parameter orientational distribution function, such as Gaussian distribution, is used.

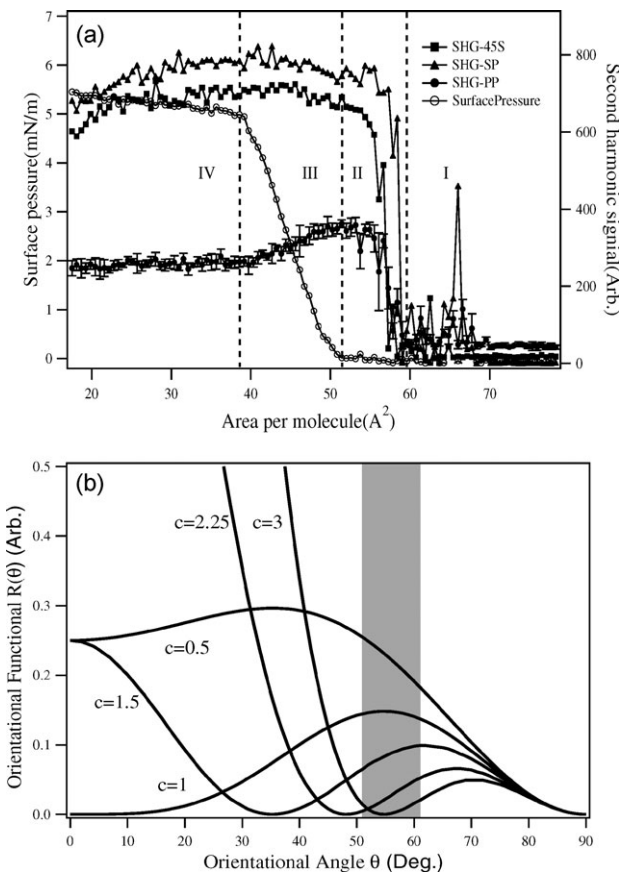

Fig. 3 (a) SHG data of the Langmuir film of the liquid crystal molecule 8CB at the air/water interface in three independent polarization combination at different surface density. The SHG wavelength is 400 nm. (b) Orientational functional $R(\theta)$ *versus* orientational angle θ with $c = 0.5$, 1, 1.5, 2.25 and 3, assuming a δ-distribution function for θ. The c values of the 8CB Langmuir monolayer in the three independent experimental polarization configuration are: $c = 1$ for s-in/p-out (*sp*) and 45°-in/*s*-out (45°s), and $c = 2.25$ for p-in/p-outb (*pp*).[56]

3.3. Effective refractive index of the interface layer

As illustrated in Fig. 1 and eqn (2.3), (2.5) and (3.6), in order to calculate c and d values for a particular SHG or SFG-VS experimental configuration, one needs to have knowledge of the interface effective refractive index $n'(\omega_i)$ for all the frequencies involved, as well as the ratios between the polarizability tensors for the chromophore under investigation.[8,47,56] Simplifications of the polarizability tensor ratios based on molecular symmetry are going to be discussed in detail in section 5. Here we discuss some general issues of the $n'(\omega_i)$.

There have been many discussions in the SHG and SFG-VS literature on the dielectric constant or refractive index of the molecular layers.[11,32,43,57,83–92] Since the interface layer is only one or several molecules thick and with certain orientational order, its dielectric properties are different from those of the bulk materials formed with the same molecule. However, for molecular monolayer or a few layers, the meaning of the refractive index or dielectric constant is not clearly defined as in the macroscopic medium. A fundamental fact in thin film optics is that the macroscopic reflection and transmission coefficients from a substrate covered with a thin molecular layer, *i.e.* thickness much smaller than the wavelength, is essentially the same as the bare interface.[93,94] Therefore, only the microscopic local field factors need to be considered. Moreover, the microscopic local field factors of this thin layer has been clearly defined to characterize the anisotropy of this oriented layer.[83] Combining these two facts, a treatment on the macroscopic Fresnel factors and microscopic local field factors, as well as the definition of the effective refractive indexes $n'(\omega_i)$ in SHG and SFG-VS, was formulated recently by Shen *et al.*[43,57] There are also other competing treatments for this ultimately important problem,[90–92] and discussions on whether a two layer model or three layer model is more suitable are also available.[89,90] However, recent quantitative analysis of SHG and SFG-VS polarization data indicates that the treatment by Shen *et al.* is not only physically clear but also quantitatively more accurate.[8,43,56,57,77] This formulation also provides a framework for the development of a molecular theory for calculating the perpendicular and parallel components of the microscopic local field factors, whose ratio gives the effective dielectric constant of the anisotropic interfacial layer.[57,83]

Because the anisotropy of the molecular layer directly determines the microscopic local field factors,[83] there is no reason to accept the notion that the effective dielectric constants in the molecular layer possess simple values,[43,57,91,92] especially for the closely packed chromophores with relatively large linear polarizability values at either the fundamental or second harmonic frequencies.[8] Theoretical modeling of the local field factors by in het Pannhuis and Munn demonstrated that improper treatment of the local fields can result in significant errors when determining the tilt angle by as much as 20° from previously obtained SHG data.[95] Since accurate orientational angles and distributions of the molecular dipoles in the molecular layer have to be known to calculate the microscopic local field factors in the thin layers, and on the other hand these factors have to be known to determine the orientational angles and distributions from SHG or the SFG-VS experimental data, this chicken-or-egg-first problem may have to be resolved through a self-consistent approach, as suggested by in het Pannhuis and Munn.[95] Therefore, there should be no general solution for this problem for different interfaces, and it has to be worked out interface by interface. Fortunately, the relative range of values for the microscopic local field factors can always be simulated,[8,83] so orientational analysis can be carried out reasonably well.[56,96] Moreover, in many cases, quantitative orientational and polarization analysis of the SHG or SFG-VS data can be used to determine the values of the microscopic local field factors.[56,97]

4. Experimental approaches for more accurate SHG measurement

Quantitative orientational and polarization analysis in SHG has to be based on accurate experimental measurements in different polarizations. Generally, such polarization measurements are realized with different wave-plate techniques.

4.1. Half-wave plate techniques *versus* quarter-wave plate techniques

Many efforts and techniques have been introduced to measure the independent susceptibilities in SHG experiments, including half-wave plate techniques[50,54,63,73,98,99] and quarter-wave plate techniques.[53,64,65,100] Recently, there are more sophisticated techniques using both half-wave plates and quarter-wave plates,[101] and even with two beams.[58,102–104] The half-wave plate techniques were used in the beginning of the development of SSHG studies.[4,51,54,105] Other techniques were developed to overcome the limitations of the half-wave plate techniques, and to study chiral interfaces.[65,100]

Half-wave plate techniques use a half-wave plate to control the linearly polarized light or SH signal in the SHG experiment. Eqn (2.4) is the general expression for half-wave plate techniques. From eqn (2.4), one can easily see that in order to unambiguously determine the relative values of the three independent susceptibilities, SHG measurements have to be made with three combinations of input and output polarizations, *i.e.* $\alpha = 0^\circ$ and $\gamma = 0^\circ$ for $\chi_{\mathrm{eff},pp}$, $\alpha = 90^\circ$ and $\gamma = 0^\circ$ for $\chi_{\mathrm{eff},sp}$, and $\alpha = 45^\circ$ and $\gamma = 90^\circ$ for $\chi_{\mathrm{eff},45^\circ s}$. However, because in the actual experiment the measured SHG intensity is proportional to $|\boldsymbol{\chi}_{\mathrm{eff}}|^2$, direct measurement with the above three polarizations can not give information of the relative sign and phase between the $\chi_{\mathrm{eff},pp}$, $\chi_{\mathrm{eff},sp}$, and $\chi_{\mathrm{eff},45^\circ s}$ terms. In order to determine the relative sign and phase between these three terms, the measurement must be made while α and γ in eqn (2.4) have other values. Thus, at least two of the three independent $\boldsymbol{\chi}_{\mathrm{eff}}$ terms can mix and interfere in one measurement.[63] In practice, the experiment is done by scanning either the α or γ angle for a full circle, *i.e.* from 0 to 360°, and in the meantime keeping the other polarization angle at a fixed value.

Considering that $\chi_{\mathrm{eff},pp}$, $\chi_{\mathrm{eff},sp}$ and $\chi_{\mathrm{eff},45^\circ s}$ are all complex, based on the half-wave plate techniques formula eqn (2.4), one has

$$|\boldsymbol{\chi}_{\mathrm{eff}}|^2 = |\chi_{\mathrm{eff}}^{\mathrm{Re}}|^2 + |\chi_{\mathrm{eff}}^{\mathrm{Im}}|^2 = |\sin^2\alpha\cos\gamma\chi_{\mathrm{eff},sp}^{\mathrm{Re}} + \sin 2\alpha\sin\gamma\chi_{\mathrm{eff},45^\circ s}^{\mathrm{Re}} + \cos^2\alpha\cos\gamma\chi_{\mathrm{eff},pp}^{\mathrm{Re}}|^2 + |\sin^2\alpha\cos\gamma\chi_{\mathrm{eff},sp}^{\mathrm{Im}} + \sin 2\alpha\sin\gamma\chi_{\mathrm{eff},45^\circ s}^{\mathrm{Im}} + \cos^2\alpha\cos\gamma\chi_{\mathrm{eff},pp}^{Im}|^2 \quad (4.12)$$

Here the real part and the imaginary part of the χ_{eff} terms never mix with each other using the half-wave plate techniques. This indicates that even though the relative signs between the real part of the three independent χ_{eff} terms can be determined, the relative signs between the real and the imaginary part can never be determined. Or, in other words, the phase between the three complex χ_{eff} terms can not be uniquely determined. This is the intrinsic limitation of the half-wave plate techniques, and this is where the quarter-wave plate techniques come to the rescue.[64,65]

The simplest case in quarter-wave plate techniques is to place a quarter-wave plate in the incident laser beam and a polarization analyzer in the outgoing beam. When the incident light before the quarter-wave plate is in *p* polarization, following the derivation in the literature,[65] we have

$$\chi_{eff} = \sin^2 2\eta \cos\gamma\chi_{eff,sp} + [\sin 4\eta + 4i \sin 2\eta]\sin\gamma\chi_{eff,45°s} + [2i \cos 2\eta - \sin^2 2\eta] \cos\gamma\chi_{eff,pp} \quad (4.13)$$

Here η is the angle between the fast axis of the quarter-wave plate and the *p* polarization.[65] Eqn (4.13) clearly shows the mixing of the real and imaginary part of the $\chi_{eff,pp}$, $\chi_{eff,sp}$ and $\chi_{eff,45°s}$ terms, and all the relative signs can be uniquely determined by fitting the experimental data with eqn (4.13). Using alternative expressions, Maki *et al*. demonstrated in their earlier works that the quarter-wave plate technique can uniquely determine all the relative values and signs between the real and imaginary terms in $\chi_{eff,sp}$, $\chi_{eff,sp}$ and $\chi_{eff,45°s}$ terms.[65]

Besides the above advantages, the quarter-wave plate technique SHG-CD is also advantageous over the half-wave plate technique SHG-LD on a chiral interface.[106,107] Recently, based on the same principles, Simpson *et al*. introduced a new modular ellipsometry approach for acquiring and interpreting polarization measurements, using multiple polarization analysis approaches, including null ellipsometry, rotating quarter-wave plate ellipsometry, and rotating half-wave plate ellipsometry.[101]

In practice, the angle η is scanned while keeping γ at a fixed value. One of the intrinsic disadvantages of the quarter-wave plate techniques is that fitting such data generally may not give accurate values for all χ_{eff} terms, because generally in the expressions such as eqn (4.13), there are many parameters and quite a few trigonometric functions involved.[65] Moreover, it is not necessary to measure the complex phase difference between the three independent χ_{eff} terms if the SHG measurement is either off-resonance or right on the resonance with the chromophore in the interface. Because in these cases, there should be no phase difference between the three independent χ_{eff} terms. In such cases, quarter-wave plate techniques offer no new information in addition to the half-wave plate measurements, except for the chiral surfaces close to molecular electronic resonance.[107–109]

Here reducing the number of fitting parameters of the polarization dependent SHG measurement is crucial for the determination of the values of the χ_{eff} terms. For example, the $|\chi_{eff,sp}|^2$ term from the non-resonant air/water interface is generally more than one order of magnitude smaller than the $|\chi_{eff,pp}|^2$ term and about one order of magnitude smaller than the $|\chi_{eff,45°s}|^2$ term.[50,73] If one scans the α with $\gamma = 45°$ (or other intermediate polarization angles), all three independent χ_{eff} terms can be fitted according to eqn (2.4) from this curve as shown in Fig. 4. However, the uncertainty of the $\chi_{eff,sp}$ term thus obtained is much larger than that from fitting the polarization curves in Fig. 5.[73] According to eqn (2.4), the approach in Fig. 4 is much more accurate because it uses two independent measurements and one trigonometric function contributing to each measurement ($\cos^2\alpha$ or $\sin 2\alpha$, respectively), compared to the single measurement of Fig. 4 which has two conjugated trigonometric functions ($\cos^2\alpha$ and $\sin 2\alpha$) contributing. Similarly, according to eqn (4.13), this problem is even more severe for the fitting with quarter-wave plate techniques, where generally at least two independent trigonometric functions ($\sin 4\eta$ and $\sin 2\eta$ when $\gamma = 90°$, or $\cos 2\eta$ and $\sin^2 2\eta$ when $\gamma = 0°$, or all four of the above when γ is neither $0°$ nor $90°$) are involved.[65,92] Therefore, in practice, the advantage of the simple half-wave plate methods in Fig. 5 may need to be reemphasized against those more complicated techniques.[58,65,92]

Besides the advantages of accurately obtaining the χ_{eff} elements, the half-wave plate techniques can also provide a direct measurement of the sign information of the χ_{eff} elements.[110] If one take the derivative of $|\chi_{eff}|^2$ from eqn (2.4) against α, when $\alpha = 0°$, one gets $2\chi_{eff,pp}\chi_{eff,45°s}\sin 2\gamma$; while when $\alpha = 90°$, one gets $-2\chi_{eff,sp}\chi_{eff,45°s}\sin 2\gamma$. Therefore, the slope of the SHG intensity against the incident polarization angle α can be used to determine the relative signs between the three independent χ_{eff} terms. Fig. 4 is the measurement of SHG intensity at 400 nm with different α angles from the air/water interface when $\gamma = 45°$. It is apparent that when $\alpha = 0°$, the slope is positive and when $\alpha = 90°$, the slope is negative. Therefore, the three χ_{eff} terms have the same signs, which is simply obtained and is fully consistent with previous measurements.[50,98,105]

The assumption that the χ_{eff} terms are in phase is valid when the molecules are not in resonance or close to resonance. Therefore, it generally covers most molecular interfaces since

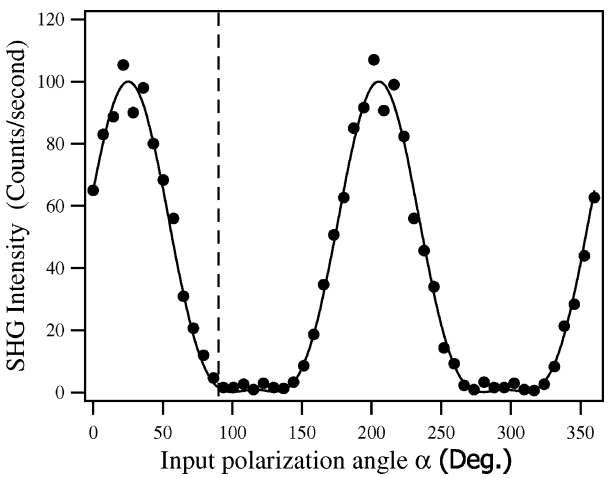

Fig. 4 Half-wave plate polarization SHG measurement of the neat air/water interface with $\gamma = 45°$. Black dots are experiment data, and the solid line is fitting with eqn (2.4). The SHG wavelength is 400 nm. The dashed line is where $\alpha = 90°$.

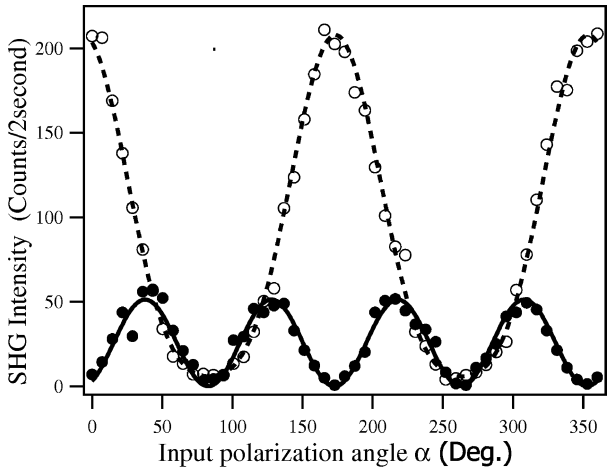

Fig. 5 Half-wave polarization SHG measurement of the neat air/water interface at two fixed detection polarizations (open circles are for $\gamma = 0°$; back dots are for $\gamma = 90°$. The SHG wavelength is 400 nm. The solid and dashed lines are fittings with eqn (2.4).[73]

in practice the ideal experimental wavelength is selective. When the three χ_{eff} terms are not in phase, the simple half-wave plate measurement can still get the relative sign between the real terms, and imaginary terms, respectively. In addition, to build the connection of relative signs between the real and imaginary terms, the quarter-wave plate techniques have to be employed.[63–65] However, as noted above, the quarter-wave plate techniques alone may cause large fitting errors for small χ_{eff} terms, and sometimes for physically unreasonable signs. This problem can be solved with the assistance of the half-wave plate techniques, which is more accurate with less fitting parameters.

The knowledge of the phase of the χ_{eff} terms can provide valuable information on molecular orientations. One can be referred to the many works on measurements of relative and absolute phase of SHG response in the literature.[63–65,100,101,111–118] The half-wave plate technique described here is one of the simplest and most direct method, and may be adequate for many applications.

4.2. Null angle method

The null angle method in the half-wave plate techniques can be used to determine whether the χ_{eff} terms are in phase or not, and it can also be used to accurately determine the magnitude of the χ_{eff} terms when they are in phase.

The null angle method in SHG was first introduced by Heinz *et al.* in 1983, later evaluated by Zhang *et al.*, and most recently reformulated by Rao *et al.*[4,54,56] This new formulation directly led to important applications in the SFG-VS studies.[8,75–77,96,119]

In the null angle method, some specific polarization set (α,γ) exists to make the SHG signal become zero (null), as long as the independent χ_{eff} terms are in phase. Therefore, the existence of such a null angle can be used as the criteria for whether the χ_{eff} terms are in phase. When they are in phase, with $\chi_{\text{eff}} = 0$ in eqn (2.4), one has,

$$\tan\gamma^{\text{null}} = \frac{\cos^2\alpha\chi_{\text{eff},pp} + \sin^2\alpha\chi_{\text{eff},sp}}{\sin(2\alpha)\chi_{\text{eff},45°s}} \tag{4.14}$$

Because γ^{null} can generally be determined very accurately, two sets of measurements at $(\alpha_1,\gamma_1^{\text{null}})$ and $(\alpha_2,\gamma_2^{\text{null}})$ can really provide an even more accurate determination of the relative magnitudes and signs of the χ_{eff} terms. Another advantage of the null angle method is that there is no ambiguity of the signs as in intensity ratio measurements.[8,56]

As shown in section 3.2, at the null angle condition, $R(\theta) = 0$, and this leads the corresponding c value to the orientational parameter D. In section 5, we show how accurately determined χ_{eff} can be used to calculate the D value using the molecular polarizability tensors of molecules with different symmetry.

5. Symmetry properties of the hyperpolarizability tensors

The molecular orientational parameter D can be determined from the accurately determined relative magnitude of the χ_{eff} terms, provided one has proper understanding of the molecular polarizability. As a 3rd rank tensor, the second order molecular polarizability $\boldsymbol{\beta}$ has 27 tensor elements in total. From Fig. 1, the ratios between all these tensor elements should be determined *a priori*. To the SHG, the number of the independent tensor elements reduce to 18 for the 'permutation symmetry'.[11,61] The number of the independent tensor elements can be reduced more with the consideration of molecular symmetry.

5.1. Achiral molecular surface ($C_{\infty v}$)

For a rotationally isotropic achiral molecular interface, two ratios between the three non-zero independent macroscopic χ_{ijk} tensor elements, namely χ_{zzz}, χ_{zxx} and χ_{xzx} can be obtained from the three independent χ_{eff} terms. Using the classification in Table 1 and eqn (2.5), one has,

$$\begin{aligned}\frac{\chi_{zxx}}{\chi_{xzx}} &= \frac{(\beta_1+\beta_2-2\beta_3)D-(\beta_1-\beta_2-2\beta_3)}{(\beta_1-\beta_2)D-(\beta_1-\beta_2-2\beta_3)}\\ \frac{\chi_{zzz}}{\chi_{xzx}} &= \frac{2(\beta_2+2\beta_3)D+2(\beta_1-\beta_2-2\beta_3)}{(\beta_1-\beta_2)D-(\beta_1-\beta_2-2\beta_3)}\end{aligned} \tag{5.15}$$

In these two equations, there are three unknown values, D and the two ratios between three β_is.

Here in Table 1 the microscopic tensors are grouped into three terms, *i.e.* β_1, β_2 and β_3. They are the only distinguishable terms related to the macroscopic tensors for the achiral isotropic interface. This classification provides a uniform formulation for molecules with different symmetry, and can greatly simplify the analysis of the SHG data.

5.2. Chiral surface (C_{∞})

There are four more non-zero elements for a chiral surface,[11,61] *i.e.* $\chi_{xyz} = \chi_{xzy} = -\chi_{yxz} = -\chi_{yzx}$. If molecule itself

Table 1 Independent non-vanishing elements of $\beta_{i'j'k'}$ for various molecular symmetries. Here the $\beta_{i'j'k'}$ tensors are classified according to their symmetry properties, and whether they appear in the macroscopic χ_{ijk} terms when the interface is with $C_{\infty v}$ symmetry. The terms in ( ) are symmetric terms which appear in the non-vanishing macroscopic susceptibility tensor terms (χ_{ijk}), terms in $\langle\ \rangle$ are asymmetric terms which appear in χ_{ijk} terms, terms in [ ] are asymmetric terms which do not appear in the χ_{ijk} terms, and terms in { } are chiral terms only for chiral molecules

			β_1, β_2, β_3 of $C_{\infty v}$ surface		
Symmetry classes	Location of mirror plane	Non-vanishing independent tensor elements	β_1	β_2	β_3
C_1	No mirror	$(\beta_{ccc}, \beta_{caa}, \beta_{cbb})$ $\langle\beta_{aca} = \beta_{aac}, \beta_{bcb} = \beta_{bbc}\rangle$ $[\beta_{aaa}, \beta_{abb}, \beta_{bab} = \beta_{bba}]$ $[\beta_{bbb}, \beta_{baa}, \beta_{aba} = \beta_{aab}]$ $[\beta_{acc}, \beta_{cac} = \beta_{cca}]$ $[\beta_{bcc}, \beta_{cbc} = \beta_{ccb}]$ $\{\beta_{cab} = \beta_{cba}, \beta_{abc} = \beta_{acb}, \beta_{bac} = \beta_{bca}\}$	β_{ccc}	$\frac{\beta_{caa}+\beta_{cbb}}{2}$	$\frac{\beta_{aca}+\beta_{bcb}}{2}$
C_{1v} (Cs)	$\hat{ac}$	$(\beta_{ccc}, \beta_{caa}, \beta_{cbb})$ $\langle\beta_{aca} = \beta_{aac}, \beta_{bcb} = \beta_{bbc}\rangle$ $[\beta_{aaa}, \beta_{abb}, \beta_{bab} = \beta_{bba}]$ $[\beta_{acc}, \beta_{cac} = \beta_{cca}]$	β_{ccc}	$\frac{\beta_{caa}+\beta_{cbb}}{2}$	$\frac{\beta_{aca}+\beta_{bcb}}{2}$
C_2	No mirror	$(\beta_{ccc}, \beta_{caa}, \beta_{cbb})$ $\langle\beta_{aca} = \beta_{aac}, \beta_{bcb} = \beta_{bbc}\rangle$ $\{\beta_{cab} = \beta_{cba}, \beta_{abc} = \beta_{acb}, \beta_{bac} = \beta_{bca}\}$	β_{ccc}	$\frac{\beta_{caa}+\beta_{cbb}}{2}$	$\frac{\beta_{aca}+\beta_{bcb}}{2}$
C_{2v}	$\hat{ac}$,$\hat{bc}$	$(\beta_{ccc}, \beta_{caa}, \beta_{cbb})$ $\langle\beta_{aca} = \beta_{aac}, \beta_{bcb} = \beta_{bbc}\rangle$	β_{ccc}	$\frac{\beta_{caa}+\beta_{cbb}}{2}$	$\frac{\beta_{aca}+\beta_{bcb}}{2}$
C_3	No mirror	$(\beta_{ccc}, \beta_{caa} = \beta_{cbb})$ $\langle\beta_{aca} = \beta_{aac} = \beta_{bcb} = \beta_{bbc}\rangle$ $[\beta_{abb} = \beta_{bab} = \beta_{bba} = -\beta_{aaa}]$ $[\beta_{aab} = \beta_{aba} = \beta_{baa} = -\beta_{bbb}]$ $\{\beta_{abc} = -\beta_{bac} = \beta_{acb} = -\beta_{bca}\}$	β_{ccc}	β_{caa}	β_{aca}
C_{3v}	$\hat{ac}$	$(\beta_{ccc}, \beta_{caa} = \beta_{cbb})$ $\langle\beta_{aca} = \beta_{aac} = \beta_{bcb} = \beta_{bbc}\rangle$ $[\beta_{abb} = \beta_{bab} = \beta_{bba} = -\beta_{aaa}]$	β_{ccc}	β_{caa}	β_{aca}
C_4, C_6, C_∞	No mirror	$(\beta_{ccc}, \beta_{caa} = \beta_{cbb})$ $\langle\beta_{aca} = \beta_{aac} = \beta_{bcb} = \beta_{bbc}\rangle$ $\{\beta_{abc} = -\beta_{bac} = \beta_{acb} = -\beta_{bca}\}$	β_{ccc}	β_{caa}	β_{aca}
C_{4v}, C_{6v}, $C_{\infty v}$	$\hat{ac}$, $\hat{bc}$	$(\beta_{ccc}, \beta_{caa} = \beta_{cbb})$ $\langle\beta_{aca} = \beta_{aac} = \beta_{bcb} = \beta_{bbc}\rangle$	β_{ccc}	β_{caa}	β_{aca}

is chiral, one has,

$$\chi_{xyz} = \chi_{xzy} = -\chi_{yxz} = -\chi_{yzx} = \frac{1}{2}N_s[\langle\cos^2\theta\rangle(\beta_{abc} - \beta_{bac}) - \frac{1}{2}\langle\sin^2\theta\rangle(\beta_{bca} - \beta_{acb})] \quad (5.16)$$

If the molecule is achiral, macroscopic chirality arises when the molecule can not rotate freely around its axis, *i.e.* the Euler angle ψ cannot be integrated,[44] one has,

$$\chi_{xyz} = \chi_{xzy} = -\chi_{yxz} = -\chi_{yzx} = \frac{1}{2}N_s[\langle\sin^2\theta\sin\psi\cos\psi\rangle(\beta_{aca} - \beta_{bcb} - \beta_{caa} + \beta_{cbb}) + \langle\sin\theta\cos\theta\sin\psi\rangle(\beta_{abb} - \beta_{acc} - \beta_{bab} + \beta_{cac}) + \langle\sin\theta\cos\theta\cos\psi\rangle(-\beta_{aba} + \beta_{baa} - \beta_{bcc} + \beta_{cbc})] \quad (5.17)$$

Experimental measurement of the chiral surfaces has not been covered above. Recently, a counterpropagating SHG experiment configuration was employed by Kriech and Conboy to directly measure the chiral χ_{xyz} term.[120–123] This measurement can be combined with the above mentioned measurements for molecular orientational analysis.

5.3. Determination and simplification of molecular polarizability tensor ratios

From eqn (5.15), two independent measurements cannot be solved for three independent variables. There are ways to simplify the number of unknown molecular polarizability tensor ratios, and one such approach was demonstrated in the analysis of the air/water interface.[73] Generally, the $\beta_{i'j'k'}$ values are dominated by a particular electronic transition. Therefore, selection rules and symmetry relations can be used to further reduce the number of non-vanishing $\beta_{i'j'k'}$. Following Moad and Simpson,[44] the non-vanishing independent β_is are listed in Table 2. For example, the lowest electronic transition of the water molecule is with B_1 or B_2 symmetry, and it dominates both ω and 2ω frequencies when far from resonance. Therefore, only β_2 and β_3 were successfully used in eqn (5.15) to solve D and the β_2/β_3 values.[73] Such simplification can also lead to intensity polarization selection rules similar to those for SFG-VS.[8]

In the SHG literature, simplification of the molecular polarizability tensor elements with uniaxial or rod-like assumptions was generally used,[21–25] except for a few cases.[16,43,51–53] From Table 2, one can clearly see why the

Table 2 Non-vanishing independent β_is in SHG for various molecular symmetries. The symmetry types of the electronic transition were catalogued by Moad and Simpson[44]

Frequency	Dominant Electronic transition	Non-vanishing β_i
2ω	A or A_1	β_1, β_2
	B or B_1 or B_2	β_3
ω	A or A_1	β_1, β_3
	B or B_1 or B_2 or E	β_2, β_3

uniaxial assumption with only non-vanishing β_{ccc} (β_1) is generally not valid.

It is also possible to employ polarization measurements in hyper Rayleigh scattering (HRS) to determine the relative ratios between some $\beta_{i'j'k'}$ tensor elements. There can be five independent polarization measurements in HRS.[124,125] Therefore, four $\beta_{i'j'k'}$ ratios can be determined. One limitation in this approach is that the relative signs of the $\beta_{i'j'k'}$ tensors can not be determined from the incoherent HRS measurement. Of course, one has to be cautioned that the hidden assumption of using HRS data for surface SHG analysis is that the polarizability tensor ratios for the molecule does not change from bulk liquid to interface.

It is clear from the expressions in eqn (5.15) that only the ratios of the β_is, instead of the ratios of the $\beta_{i'j'k'}$s, are crucial for orientational analysis. Therefore, there is no need to get the ratios between each individual $\beta_{i'j'k'}$ for interpretation of the SHG data. Molecular calculations have been employed to obtain the $\beta_{i'j'k'}$ tensor values. The results are generally scattered and hard to verify experimentally.[126–129] Through above symmetry analysis, such complications can be generally avoided. In conclusion, above formulation not only provides a uniform description, but also significantly simplifies the polarization and orientational analysis in dealing with SHG experimental data.

6. Surface *vs.* bulk contribution: air/water interface as the benchmark case

The precondition for the application of SHG in interface studies is its interface specificity.

In the early days of the development of SHG for interface studies, great efforts have been made to assess the relative magnitudes of the interface (local) contribution and the still possibly significant bulk electric quadrupole and magnetic dipole (nonlocal) contributions to the SHG signal.[11,130–132] Even though there were debates on whether SHG can be an effective probe for isotropic liquid interfaces, *i.e.* whether the bulk contributions is negligible,[133–137] it has been generally accepted that it is impossible to separate the bulk contribution from the total SHG signal.[32,132,133] Over the past two decades, theoretical treatment has shown that there is no general solution to this problem, and it is often not known *a priori* in SSHG and SFG-VS studies whether interfacial contribution is dominant over that of the bulk in an interface system or not.[138–140] Among these studies, the SHG from the air/water interface is the most studied, and it is also the benchmark case favoring significant bulk (non-local) contributions.[50,98,99,105]

In a very recent work,[73] through the detailed analysis of accurately measured SHG data from the air/water interface, it was found that all the previous experimental evidences favoring significant bulk (non-local) contributions, *i.e.* the breaking of the Kleinman symmetry and the temperature dependence of the SHG signal, were invalid. This development was based on a proof of the equivalence of the macroscopic and the microscopic (molecular) Kleinman symmetry under rotational (Euler) transformation.[73] From Table 2, one can see that the microscopic Kleinman symmetry ($\beta_2 = \beta_3$) is generally not observed for any realistic molecule according to the dispersion relationships.[141,142] Therefore, since it is easy to prove that the $\beta_{i'j'k'}$ of individual water molecule does not preserve the Kleinman symmetry,[142] the breaking of the macroscopic Kleinman symmetry from the air/water interface can not be used as the support for bulk (non-local) contributions. With the accurate measurements of the SHG signal from the air/water interface as described in section 4, and the symmetry analysis described in section 5, all SHG data from the air/water interface can be interpreted without introducing any bulk (non-local) contributions.[73] Even though logically this treatment is impossible to be considered as a complete proof, this development strongly suggests an insignificant bulk contribution for SHG from the air/water interface.

This new treatment of the SHG from the air/water interface indicates the importance of accurate polarization measurement and the power of symmetry analysis of the polarizability tensors. This effort directly led to the discussions and formulations in sections 4 and 5. Based on these new methodologies and understandings, quantitative re-examination of SHG data on other important systems can be carried out. Such efforts shall put SHG interface studies on an even more solid foundation. Nevertheless, the successful treatment of the neat air/water interface with dipole contribution terms indicates that SHG probably is indeed an effective probe of the surfaces and interfaces of isotropic fluids, as strongly argued by Andrews *et al.*[68,69,134,136,137]

7. Conclusion and perspectives

This review focuses on the recent advances on quantitative measurement and interpretation of SHG from the achiral rotationally isotropic molecular interfaces and thin films. There have been a number of excellent reviews on the theoretical basis and applications of SHG in interface studies in the literatures. Since the ability to apply SHG to molecular interface studies depends on the ability to abstract quantitative information from the measurable quantities in the actual SHG experiments, this review may help to fill the gap for a better understanding and application of SHG to surface studies through the discussion of the issues directly related to accurate experimental measurement and quantitative interpretation of the SHG data. Therefore, this review may also be viewed as a contemporary footnote to the century old quotation generally attributed to the great Lord Kelvin: 'Unless our knowledge is measured and expressed in numbers, it does not amount to much'.

In this review, we discussed the methodologies for orientational analysis of the SHG experimental data, the experimental approaches crucial for accurate SHG measurements, and a systematic treatment of the molecular polarizability tensors based on their symmetry properties in association with the experimentally measurable quantities. The importance and approaches of the treatment on the local field factors for obtaining quantitative information was also discussed. In the end, the problem of surface *versus* bulk contribution in SHG surface studies was also presented. These developments may provide a rather unified formulation for quantitative application of SHG in molecular interfaces and thin films studies.

There are many issues and topics in surface SHG studies not covered in this review. Some of these topics are SHG from micro- and nanoparticles, as well as colloidal surfaces, SHG from metal or semiconductor surfaces, SHG from chiral surfaces, SHG from magnetic films, *etc*. Interested readers can be referred to many existing reviews on such topics, and developments using approaches presented in this review are expected in the future studies.

Acknowledgements

HFW thanks supports by the Natural Science Foundation of China (NSFC, No. 20373076, No. 20425309, No. 20533070).

References

1 Y. R. Shen, *The Principles of Nonlinear Optics*, Wiley, New York, 2003.
2 C. K. Chen, A. R. B. Decastro and Y. R. Shen, *Phys. Rev. Lett*., 1981, **46**, 145.
3 T. F. Heinz, C. K. Chen, D. Ricard and Y. R. Shen, *Phys. Rev. Lett*., 1982, **48**, 478.
4 T. F. Heinz, H. W. K. Tom and Y. R. Shen, *Phys. Rev. A*, 1983, **28**, 1883.
5 Y. R. Shen, *J. Vac. Sci. Technol., B*, 1985, **3**, 1464.
6 X. D. Zhu, H. Suhr and Y. R. Shen, *Phys. Rev. B*, 1987, **35**, 3047.
7 P. Guyot-Sionnest, R. Superfine, J. H. Hunt and Y. R. Shen, *Chem. Phys. Lett*., 1988, **144**, 1.
8 H. F. Wang, W. Gan, R. Lu, Y. Rao and B. H. Wu, *Int. Rev. Phys. Chem*., 2005, **24**, 191.
9 G. L. Richmond, J. M. Robinson and V. L. Shannon, *Prog. Surf. Sci*., 1988, **28**, 1.
10 Y. R. Shen, *Nature*, 1989, **337**, 519.
11 Y. R. Shen, *Annu. Rev. Phys. Chem*., 1989, **40**, 327.
12 G. J. Simpson and K. L. Rowlen, *Acc. Chem. Res*., 2000, **33**, 781.
13 G. J. Simpson, *Appl. Spectrosc*., 2001, **55**, 16A.
14 G. J. Blanchard, *Appl. Spectrosc*., 2001, **55**, 110A.
15 K. B. Eisenthal, *Acc. Chem. Res*., 1993, **26**, 636.
16 R. M. Corn and D. A. Higgins, *Chem. Rev*., 1994, **94**, 107.
17 K. B. Eisenthal, *Chem. Rev*., 1996, **96**, 1343.
18 Y. R. Shen, *Annu. Rev. Mater. Sci*., 1986, **16**, 69.
19 S. Sioncke, T. Verbiest and A. Persoons, *Mater. Sci. Eng., R*, 2003, **42**, 115.
20 M. Chen, L. R. Dalton, L. P. Yu, Y. Q. Shi and W. H. Steier, *Macromolecules*, 1992, **25**, 4032.
21 G. J. Ashwell, R. C. Hargreaves, C. E. Baldwin, G. S. Bahra and C. R. Brown, *Nature*, 1992, **357**, 393.
22 G. J. Ashwell, P. D. Jackson and W. A. Crossland, *Nature*, 1994, **368**, 438.
23 G. J. Ashwell, G. Jefferies, D. G. Hamilton, D. E. Lynch, M. P. S. Roberts, G. S. Bahra and C. R. Brown, *Nature*, 1995, **375**, 385.
24 S. B. Roscoe, A. K. Kakkar, T. J. Marks, A. Malik, M. K. Durbin, W. P. Lin, G. K. Wong and P. Dutta, *Langmuir*, 1996, **12**, 4218.
25 G. J. Ashwell, G. Jefferies, C. D. George, R. Ranjan, R. B. Charters RB and R. P. Tatam, *J. Mater. Chem*., 1996, **346**, 131.
26 Y. Lvov, S. Yamada and T. Kunitake, *Thin Solid Films*, 1997, **300**, 107.
27 C. P. Collier, R. J. Saykally, J. J. Shiang, S. E. Henrichs and J. R. Heath, *Science*, 1997, **277**, 1978.
28 T. Petralli, T. M. Wong, J. D. Byers, H. I. Yee and J. M. Hicks, *J. Phys. Chem*., 1993, **97**, 1383.
29 H. F. Wang, E. Borguet and K. B. Eisenthal, *J. Phys. Chem. A*, 1997, **101**, 713.
30 H. F. Wang, E. Borguet and K. B. Eisenthal, *J. Phys. Chem. B*, 1998, **102**, 4927.
31 P. B. Petersen and R. J. Saykally, *Annu. Rev. Phys. Chem*., 2006, **57**, 333.
32 T. F. Heinz, *Nonlinear Optical Effects at Surfaces and Interfaces in Nonlinear Surface Electromagnetic Phenomena*, ed. H. E. Ponath and G. I. Stegman, North-Holland, Amsterdam, 1991, pp. 353–416.
33 P. F. Brevet, *Surface Second Harmonic Generation*, Press Polytechniques et Universitaires Romandes, Lausanne, 1997.
34 H. F. Wang, E. C. Y. Yan, E. Borguet and K. B. Eisenthal, *Chem. Phys. Lett*., 1996, **259**, 15.
35 K. B. Eisenthal, *Chem. Rev*., 2006, **106**, 1462.
36 P. Figliozzi, L. Sun, Y. Jiang, N. Matlis, B. Mattern, M. C. Downer, S. P. Withrow, C. W. White, W. L. Mochán and B. S. Mendoza, *Phys. Rev. Lett*., 2005, **94**, 047401.
37 M. Florsheimer, M. Bosch, Ch. Brillert, M. Wierschem and H. Fuchs, *Supramol. Sci*., 1997, **4**, 255.
38 R. Gauderon, P. B. Lukins and C. J. R. Sheppard, *Micron*, 2001, **32**, 691.
39 S. Yamada and I. Y. S. Lee, *Anal. Sci*., 1998, **14**, 1045.
40 G. J. Simpson, *ChemPhysChem*, 2004, **5**, 1301.
41 P. Fischer and F. Hache, *Chirality*, 2005, **17**, 42.
42 M. A. Belkin and Y. R. Shen, *Int. Rev. Phys. Chem*., 2005, **24**, 257.
43 X. Zhuang, P. B. Miranda, D. Kim and Y. R. Shen, *Phys. Rev. B*, 1999, **59**, 12632.
44 A. J. Moad and G. J. Simpson, *J. Phys. Chem. B*, 2004, **108**, 3548.
45 G. J. Simpson, J. M. Perry and C. L. Ashmore-Good, *Phys. Rev. B*, 2002, **66**, 165437.
46 R. Lu, W. Gan, B. H. Wu, H. Chen and H. F. Wang, *J. Phys. Chem. B*, 2004, **108**, 7297.
47 R. Lu, W. Gan, B. H. Wu, Z. Zhang, Y. Guo and H. F. Wang, *J. Phys. Chem. B*, 2005, **109**, 14118.
48 W. Gan, D. Wu, Z. Zhang, Y. Guo and H. F. Wang, *Chin. J. Chem. Phys*., 2006, **19**, 20.
49 W. Gan, D. Wu, Z. Zhang, R. R. Feng and H. F. Wang, *J. Chem. Phys*., 2006, **124**, 114705.
50 A. J. Fordyce, W. J. Bullock, A. J. Timson, S. Haslam, R. D. Spencer-Smith, A. Alexander and J. G. Frey, *Mol. Phys*., 2001, **99**, 677.
51 D. A. Higgins, S. K. Byerly, M. B. Abrams and R. M. Corn, *J. Phys. Chem*., 1991, **95**, 6984.
52 D. A. Higgins, M. B. Abrams, S. K. Byerly and R. M. Corn, *Langmuir*, 1992, **8**, 1994.
53 S. A. Mitchell, *J. Phys. Chem. B*, 2006, **110**, 883.
54 T. G. Zhang, C. H. Zhang and G. K. Wong, *J. Opt. Soc. Am. B*, 1990, **7**, 902.
55 M. B. Feller, W. Chen and Y. R. Shen, *Phys. Rev. A*, 1991, **43**, 6778.
56 Y. Rao, Y. S. Tao and H. F. Wang, *J. Chem. Phys*., 2003, **119**, 5226.
57 X. Wei, S. C. Hong, X. W. Zhuang, T. Goto and Y. R. Shen, *Phys. Rev. E*, 2000, **62**, 5160.
58 S. Cattaneo, E. Vuorimaa, H. Lemmetyinen and M. Kauranen, *J. Chem. Phys*., 2004, **120**, 9245.
59 H. F. Wang, *Chin. J. Chem. Phys*., 2004, **17**, 362.
60 H. Goldstein, *Classical Mechanics*, Addison-Wesley Publishing Company Inc., Reading, MA, 1980, pp. 147.
61 P. Fischer and A. D. Buckingham, *J. Opt. Soc. Am. B*, 1998, **15**, 2951.
62 C. D. Bain, *J. Chem. Soc., Faraday Trans*., 1995, **91**, 1281.
63 O. Roders, O. Befort, G. Marowsky, D. Mobius and A. Bratz, *Appl. Phys. B*, 1994, **59**, 537.
64 F. Geiger, R. Stolle, G. Marowsky, M. Palenberg and B. U. Felderhof, *Appl. Phys. B*, 1995, **61**, 135.
65 J. J. Maki, M. Kauranen, T. Verbiest and A. Persoons, *Phys. Rev. B*, 1997, **55**, 5021.
66 J. F. Ward, *Rev. Mod. Phys*., 1965, **37**, 1.
67 G. J. Simpson, J. M. Perry and C. L. Ashmore-Good, *Phys. Rev. B*, 2002, **66**, 165437.
68 P. Allcock, D. L. Andrews, S. R. Meech and A. J. Wigman, *Phys. Rev. A*, 1996, **53**, 2788.
69 D. L. Andrews and L. D. Romero, *J. Phys. B: At. Mol. Opt. Phys*., 2001, **34**, 2177.
70 G. J. Simpson and K. L. Rowlen, *J. Am. Chem. Soc*., 1999, **121**, 2635.
71 G. J. Simpson and K. L. Rowlen, *Anal. Chem*., 2000, **72**, 3399.
72 G. J. Simpson and K. L. Rowlen, *Anal. Chem*., 2000, **72**, 3407.
73 W. K. Zhang, D. S. Zheng, Y. Y. Xu, H. T. Bian, Y. Guo and H. F. Wang, *J. Chem. Phys*., 2005, **123**, 224713.

74 G. J. Simpson, S. G. Westerbuhr and K. L. Rowlen, *Anal. Chem.*, 2000, **72**, 887.
75 H. Chen, W. Gan, R. Lu, Y. Guo and H. F. Wang, *J. Phys. Chem. B*, 2005, **109**, 8053.
76 H. Chen, W. Gan, R. Lu, Y. Guo and H. F. Wang, *J. Phys. Chem. B*, 2005, **109**, 8064.
77 W. Gan, B. H. Wu, H. Chen, Y. Guo and H. F. Wang, *Chem. Phys. Lett.*, 2005, **406**, 467.
78 J. Z. Xue, C. S. Jung and M. W. Kim, *Phys. Rev. Lett.*, 1992, **69**, 474.
79 Th. Enderle, A. J. Meixner and I. Zschokke-Granacher, *J. Chem. Phys.*, 1994, **101**, 4365.
80 G. A. Sefler, Q. Du, P. B. Miranda and Y. R. Shen, *Chem. Phys. Lett.*, 1995, **235**, 347.
81 T. G. Zhang, Z. M. Feng, G. K. Wong and J. B. Ketterson, *Langmuir*, 1996, **12**, 2298.
82 S. J. McGall, P. B. Davies and D. J. Neivandt, *J. Phys. Chem. B*, 2003, **107**, 4718.
83 P. X. Ye and Y. R. Shen, *Phys. Rev. B*, 1983, **28**, 4288.
84 G. Cnossen, K. E. Drabe and D. A. Wiersma, *J. Chem. Phys.*, 1992, **97**, 4512.
85 R. W. Munn, *J. Chem. Phys.*, 1992, **97**, 4532.
86 M. in het Panhuis and R. W. Munn, *J. Chem. Phys.*, 2000, **113**, 10685.
87 R. Braun, B. D. Casson and C. D. Bain, *Chem. Phys. Lett.*, 1995, **245**, 326.
88 M. B. Feller, W. Chen and Y. R. Shen, *Phys. Rev. A*, 1991, **43**, 6778.
89 F. Eisert, O. Dannenberger and M. Buck, *Phys. Rev. B*, 1998, **58**, 10860.
90 D. Roy, *Phys. Rev. B*, 2000, **61**, 13283.
91 J. G. Frey, *Chem. Phys. Lett.*, 2000, **323**, 454.
92 G. J. Simpson, C. A. Dailey, R. M. Plocinik, A. J. Moad, M. A. Polizzi and R. M. Everly, *Anal. Chem.*, 2005, **77**, 215.
93 R. M. A. Azzam and N. M. Bashara, *Ellipsometry and Polarized Light*, Elsevier, Amsterdam, 1987.
94 O. S. Heavens, *Optical Properties of Thin Solid Films*, Dover Publications Inc., New York, 1991.
95 M. in het Panhuis and R. W. Munn, *J. Chem. Phys.*, 2000, **113**, 10691.
96 H. Chen, W. Gan, B. H. Wu, D. Wu, Z. Zhang and H. F. Wang, *Chem. Phys. Lett.*, 2005, **408**, 284.
97 Y. Rao, D. S. Zheng and H. F. Wang, unpublished work.
98 A. A. T. Luca, P. Hebert, P. F. Brevet and H. H. Girault, *J. Chem. Soc., Faraday Trans.*, 1995, **91**, 1763.
99 R. Antoine, F. Bianchi, P. F. Brevet and H. H. Girault, *J. Chem. Soc., Faraday Trans.*, 1997, **93**, 3833.
100 S. K. Andersson, M. C. Schanne-Klein and F. Hache, *Phys. Rev. B*, 1999, **59**, 3210.
101 R. M. Plocinik, R. M. Everly, A. J. Moad and G. J. Simpson, *Phys. Rev. B*, 2005, **72**, 125409.
102 S. Cattaneo and M. Kauranen, *Opt. Lett.*, 2003, **28**, 1445.
103 P. Figliozzi, L. Sun, Y. Jiang, N. Matlis, B. Mattern, M. C. Downer, S. P. Withrow, C. W. White, W. L. Mochan and B. S. Mendoza, *Phys. Rev. Lett*, 2005, **94**, 047401.
104 S. Cattaneo and M. Kauranen, *Phys. Rev. B*, 2005, **72**, 033412.
105 M. C. Goh, J. M. Hicks, K. Kemnitz, G. R. Pinto, K. Bhattacharyya, K. B. Eisenthal and T. F. Heinz, *J. Phys. Chem.*, 1988, **92**, 5074.
106 T. Verbiest, M. Kauranen and A. Persoons, *J. Opt. Soc. Am. B*, 1998, **15**, 451.
107 J. J. Maki, T. Verbiest, M. Kauranen, S. V. Elshocht and A. Persoons, *J. Chem. Phys.*, 1996, **105**, 767.
108 J. M. Hicks and T. Petralli-Mallow, *Appl. Phys. B*, 1999, **68**, 589.
109 M. A. Belkin, S. H. Han, X. Wei and Y. R. Shen, *Phys. Rev. Lett.*, 2001, **87**, 113001.
110 D. S. Zheng and H. F. Wang, unpublished work.
111 R. K. Chang, J. Ducuing and N. Bloembergen, *Phys. Rev. Lett.*, 1965, **15**, 6.
112 K. Kemnitz, K. Bhattacharyya, J. M. Hicks, G. R. Pinto and K. B. Eisenthal, *Chem. Phys. Lett.*, 1986, **131**, 285.
113 G. Berkovic, Y. R. Shen, G. Marowsky and R. Steinhoff, *J. Opt. Soc. Am. B*, 1989, **6**, 205.
114 O. Sato, R. Baba, K. Hashimoto and A. Fujishima, *J. Phys. Chem.*, 1991, **95**, 636.
115 K. J. Veenstra, A. V. Petukhov, A. P. de Boer and Th. Rasing, *Phys. Rev. B*, 1998, **58**, R16020.
116 H. Kimura-Suda, T. Sassa, T. Wada and H. Sasabe, *J. Phys. Chem. B*, 2001, **105**, 1763.
117 R. Lu, Y. Rao, W. K. Zhang and H. F. Wang, *Proc. SPIE-Int. Soc. Opt. Eng.*, 2002, **4812–15**, 115.
118 R. Lu and H. F. Wang, *Chin. Phys. Lett.*, 2003, **20**, 1269.
119 (*a*) R. Lu, W. Gan and H. F. Wang, *Chin. Sci. Bull.*, 2003, **48**, 2183; (*b*) R. Lu, W. Gan and H. F. Wang, *Chin. Sci. Bull.*, 2004, **49**, 899.
120 M. A. Kriech and J. C. Conboy, *J. Opt. Soc. Am. B*, 2004, **21**(5), 1013.
121 M. A. Kriech and J. C. Conboy, *J. Am. Chem. Soc.*, 2003, **125**, 1148.
122 M. A. Kriech and J. C. Conboy, *J. Am. Chem. Soc.*, 2005, 2834.
123 M. A. Kriech and J. C. Conboy, *Appl. Spectrosc.*, 2005, **127**, 746.
124 R. Bersohn, Y. H. Pao and H. L. Frisch, *J. Chem. Phys.*, 1966, **45**, 3184.
125 S. F. Hubbard, R. G. Petschek, K. D. Singer, N. D. Sidocky, C. Hudson, L. C. Chien, C. C. Henderson and P. A. Cahill, *J. Opt. Soc. Am. B*, 1998, **15**, 289.
126 Y. Luo, H. Ågren, O. Vahtras, P. Jørgensen, V. Spirko and H. Hettema, *J. Chem. Phys.*, 1993, **98**, 7159.
127 K. O. Sylvester-Hvid, K. V. Mikkelsen, D. Jonsson, P. Norman and H. Ågren, *J. Chem. Phys.*, 1998, **109**, 5576.
128 G. Maroulis, *J. Chem. Phys.*, 2000, **113**, 1813.
129 J. Kongsted, A. Osted, K. V. Mikkelsen and O. Christiansen, *J. Chem. Phys.*, 2003, **119**, 10519.
130 P. Guyot-Sionnest, W. Chen and Y. R. Shen, *Phys. Rev. B*, 1986, **33**, 8254.
131 P. Guyot-Sionnest and Y. R. Shen, *Phys. Rev. B*, 1987, **35**, 4420.
132 P. Guyot-Sionnest and Y. R. Shen, *Phys. Rev. B*, 1988, **38**, 7985.
133 T. F. Heinz and D. P. Divincenzo, *Phys. Rev. A*, 1990, **42**, 6249.
134 D. L. Andrews and N. P. Blake, *Phys. Rev. A*, 1988, **38**, 3113.
135 X. D. Zhu and Y.R. Shen, *Phys. Rev. A*, 1990, **41**, 4549.
136 D. L. Andrews and N. P. Blake, *Phys. Rev. A*, 1990, **41**, 4550.
137 D. L. Andrews, *J. Mod. Opt.*, 1993, **40**, 939.
138 Y. R. Shen, *Appl. Phys. B*, 1999, **68**, 295.
139 X. Wei, S.-C. Hong, A. I. Lvovsky, H. Held and Y. R. Shen, *J. Phys. Chem. B*, 2000, **104**, 3349.
140 H. Held, A. I. Lvovsky, X. Wei and Y. R. Shen, *Phys. Rev. B*, 2002, **66**, 205110.
141 C. A. Dailey, B. J. Burke and G. J. Simpson, *Chem. Phys. Lett.*, 2004, **390**, 8.
142 P. A. Franken and J. F. Ward, *Rev. Mod. Phys.*, 1963, **35**, 23.

